

EVALUATING THE ACCURACY OF SATELLITE DERIVED BATHYMETRY

Ratna Sari Dewi, Prayudha Hartanto, Yustisi Lumban-Gaol, Aldino Rizaldy, Ayu Nur Syafii, Nadya Oktaviani, Intan Pujawati, Nursugi, Ati Rahadiati and Sandi Aditya

¹ Geospatial Information Agency (Badan Informasi Geospasial),
Jl. Raya Jakarta-Bogor Km. 46, Cibinong, Bogor, 16911 – Indonesia

Email: ratna.sari@big.go.id; prayudha.hartanto@big.go.id; yustisi.ardhitasari@big.go.id; aldino.rizaldy@big.go.id; ayunursafii.10@gmail.com; nadya.oktaviani@big.go.id; intan.pujawati@big.go.id; nursugi@big.go.id; ati.rahadiati@big.go.id and sandi.aditya@big.go.id

KEY WORDS: bathymetry, depth, satellite-derived bathymetry, Morotai

ABSTRACT: Satellite remote sensing enable the collection of high-resolution bathymetry data to be integrated by terrestrial information in order to develop coastal terrain models and shoreline model. Satellite derived bathymetry is promising due to its ability to fill the gap of depth obtained from hydrographic survey. This research focused on developing a bathymetric model of small islands in Morotai, Indonesia. The model was created using depth derived from satellite imagery to provide data in the near-shore gap between sea level and the beginning of sonar data. A semi-parametric generalized linear model (GAM) was applied and combined echo-sounding measurements and the reflectance of blue, green, and red of four satellite images (World View 2, Kompsat 3A, Sentinel 2A and Landsat 8) were used. We evaluated the accuracy of the algorithm and compare it with Multi-linear Regression. From the results, we found that GAM outperformed MLR in deriving depth information. Furthermore, the use of finer resolution images also increased the accuracy of SDB model. The accuracies range from 0.9-1.9 when applying GAM using WorldView-2 while when applying MLR, the accuracies range from 1.9-5.3.

1. INTRODUCTION

Accurate satellite derived bathymetry is considered of fundamental aspect towards monitoring sea floor and deriving nautical charts to support marine navigation. Collecting depth information in particular for shallow water area has been done mainly by using bathymetric surveying, for i.e., ship-borne echo sounding measurements and LIDAR (Light Detection and Ranging) data. However, these techniques are costly both in time and money. Moreover, the first technique is constrained by ship access and safety reason (Pattanaik et al., 2015), while LIDAR for bathymetry is very expensive (Kanno et al., 2013).

Considering those limitations, extracting depth information from remote sensing data has been an option during last decades. Satellite derived bathymetry provides a cost and time effective solution for a relatively accurate bathymetry data. The initial research on the estimation of water depth was started by Lyzenga (1978) in 1978. With the widely available of remote sensing data, the methods on monitoring sea bottom were increased so that it can be applied by many researchers such as Philpot (1989), Kanno et al. (2013), Stumpf et al. (2003) and Chénier et al. (2018).

This research aims to evaluate the accuracy of three methods in deriving depth information from remote sensing data which was tested in shallow water area of a small island in Morotai, Indonesia. For this research, multi spectral imageries from four sensors were used. In this case, comparisons between two SDB techniques as well as accuracy assessments using available bathymetric data were done in order to identify approaches that have the best performance given the environmental conditions of the study site at the time of image acquisition.

2. STUDY AREA AND DATASET

2.1 Study Area

This research focuses on deriving bathymetry for a small island located at the south-western part of Morotai Island coastal area (Figure 1). The central point of the study area is at geographical coordinates 2° 7' 30" N and

128° 13' 23" E. Morotai Island is the northernmost island in Indonesia. It is surrounded by many small islands and is one of the tourist destinations located in North Maluku Province since it has clear water with stunning white sandy beaches. It has beautiful underwater scenery with coral reef formation and sea grass (Hengky, 2017; Saputro et al., 2012).

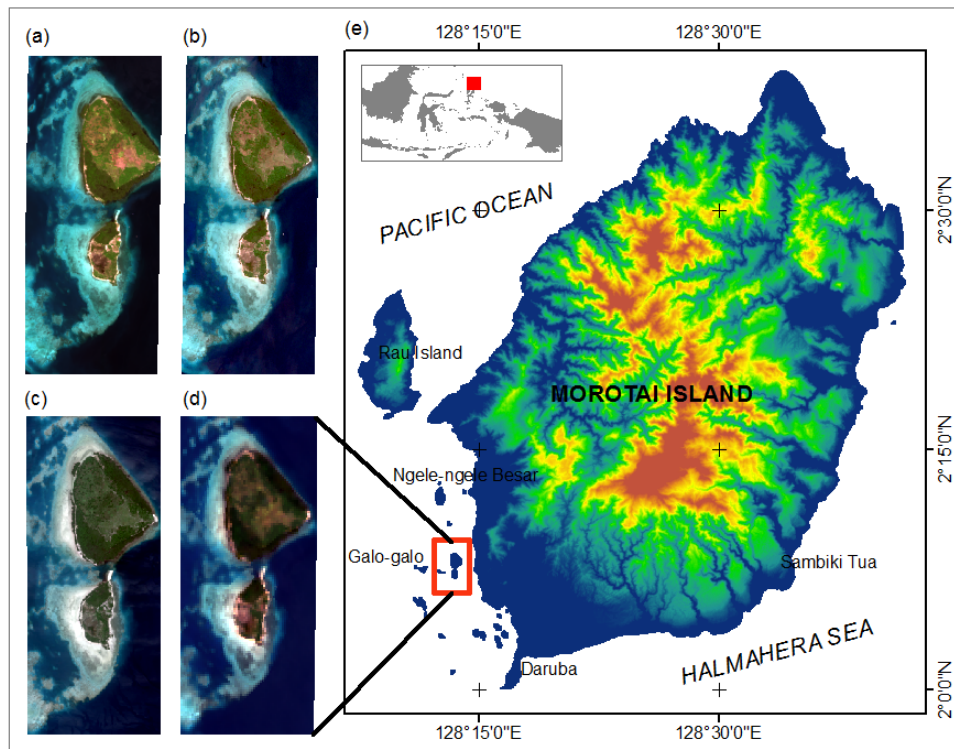


Figure 1. Study area in a small island located at the south-western part of Morotai Island coastal area, North Maluku Province, Indonesia. Four datasets from four satellite imageries, namely: a) WorldView-2, b) Kompsat-3, c) Sentinel-2A, and d) Landsat 8 OLI/TIRS are used to estimate depth information, and true color composite is used as background in Figure 1a-d (green pixels represent vegetation, red-brown pixels are built-up, dark blue pixels are water, white bluish pixels are mixed of water and sand, and white pixels are sand). Red rectangle shows the study area location.

2.2 Remote sensing dataset

The satellite data sets from four different sensors were used in this study. Information regarding images used in this research is provided in Table 1. Specifications of each satellite images are described as follows:

WorldView-2: WorldView-2 image was recorded in 21 February 2015 with 2 m spatial resolution. The image was obtained from Indonesia Geospatial Information Agency (BIG) in Ortho Ready Standard (OR2A) product. It means the product is map projected without topographic relief applied with respect to the reference ellipsoid (DigitalGlobe, 2013) and is radiometrically corrected and sensor corrected. Four spectral bands were used to estimate depth information in this study, namely blue (0.44-0.51 μm), green (0.51-0.58 μm), red (0.62-0.69 μm), and near infrared (0.77-0.90 μm) parts of the spectrum (DigitalGlobe, 2019).

Kompsat-3: Kompsat-3 (Korean Multi-Purpose Satellite) was developed by the Korea Aerospace Research Institute (KARI) and launched on 17 May 2012. The image was recorded in 16 June 2016 with 2.8 m spatial resolution. This image was obtained from Posco International Corporation (Indonesia Representative Office) in Level 1G product which is corrected for geometric distortion and projected to UTM. This Level 1G includes all radiometric corrections and sensor corrections. However, terrain effects are corrected using coarse DEM, namely SRTM DEM. For this study, only four spectral bands that were used for SDB estimation, for i.e., blue (0.45-0.52 μm), green (0.52-0.6 μm), red (0.63-0.69 μm), and near infrared (0.76-0.9 μm) parts of the spectrum (KARI, 2015).

Sentinel 2A: The Sentinel-2A image was obtained freely from The Copernicus Open Access (ESA, 2019) in level L2A. The time acquisition of the image was in 21 May 2019 with 10 m spatial resolution. For this research, we used only four bands of Sentinel 2A: blue (0.49 μm), green (0.56 μm), red (0.665 μm), and near infrared (0.842

μm) parts of the spectrum (ESA, 2015). Sentinel-2A adopted for this study was in Level-2A product which is provided with Bottom of Atmosphere (BoA) reflectance. A standard radiometric and geometric corrections including the orthorectification with sub-pixel accuracies (SUHET, 2015)

Landsat 8 OLI/TIRS: Landsat has a 16-day revisit time and passes Indonesia at approximately 02.00-03.00 GMT. The images are available freely from USGS (2019b). For this study, we used Landsat 8 OLI/TIRS which was recorded in 20 February 2019 with 30 m spatial resolution. Only four spectral bands of this image were applied to the SDB model, namely the blue (0.45–0.515 μm), green (0.525–0.605 μm), red (0.63–0.69 μm), and near infrared (0.75–0.90 μm) parts of the electromagnetic spectrum (USGS, 2019a). For the purpose of SDB extraction, we used Landsat image that was in the surface reflectance format. The image has been implemented a standard radiometric and geometric corrections including the orthorectification with sub-pixel accuracies (USGS, 2019a).

Table 1. Images used for bathymetry extraction in this study

Sensors	Acquisition Date	Resolution (m)
WorldView-2	21-02-2015	2
Kompsat-3	16-06-2016	2.8
Sentinel-2A	21-05-2019	10
Landsat 8 OLI/TIRS	20-02-2019	30

2.3 Bathymetry data

Single Beam Echo Sounder (SBES) is used to build and validate the models. The SBES was collected in August 2018. In order to have zero tides influence, tide correction was applied to the data. The depth information ranges from 3 m up to 30 m. For the implementation of the SDB model, we selected randomly 25% of training data from the SBES measurement points. The reason of this selection was that we would like to test the capability of each algorithm by using a minimum training data. Further, we evaluated the accuracy of SDB model by using 75% of SBES points.

3. METHODOLOGY

3.1 Pre-processing of images

Before applying SDB algorithm to estimate depth information, we applied dark object subtraction method to the images using ENVI software. For each image, five datasets were created; the first dataset consists of four bands in blue, green, red, and near infrared bands (visible plus near infrared/NIR bands); the second dataset consist of three bands in blue, green, and red bands; the rest scenarios only use two visible bands, i.e., blue and green, blue and red, and green and blue bands. By using these scenarios, we would like to test which band combinations obtain a better result of depth information.

Based on assumption from Kanno (2011) and Vinayaraj et al. (2016), spectral radiance (λ_s) in shallow water observed by a sensor is consisting four elements: atmospheric scattering (λ_a), reflection of sea surface (λ_r), in-water scattering (λ_w), and bottom reflection (λ_b) (see Figure 2). Therefore, the observed spectral radiance in shallow water (L_s) can be expressed by a function of wavelength as:

$$\lambda_s = \lambda_a + \lambda_r + \lambda_w + \lambda_b \quad (1)$$

As part of image preprocessing, water correction method was applied to those images based on Lyzenga (1981) and Gholamalifard et al. (2013). The methods assumed that there is no variation of sea-surface and atmospheric scattering over the water area and that in the deep water, there is no bottom reflectance element in the spectral radiance observed by the sensor. Since the deep water has a low spectral value, we can estimate the transformed radiance (λ_s) from spectral properties of this deep area by making another assumption that the reflectance is solely due to scattering. Thus, we can estimate the average value of pixels in the deep water and transformed the measured radiance as follows (Gholamalifard et al., 2013):

$$Y_i = \log(\lambda)_i - \text{mean}(\lambda_d)_i \quad (2)$$

$(\lambda_s)_i$ is the measured radiance in shallow water for band i and $(\lambda_d)_i$ is the radiance in the deep water. The transformed radiance value (Y_i) is linear function of the water depth since it shows a linear relation between

spectral value in shallow water and deep water. By using this formula, we removed the influence of atmospheric and sea-surface scattering.

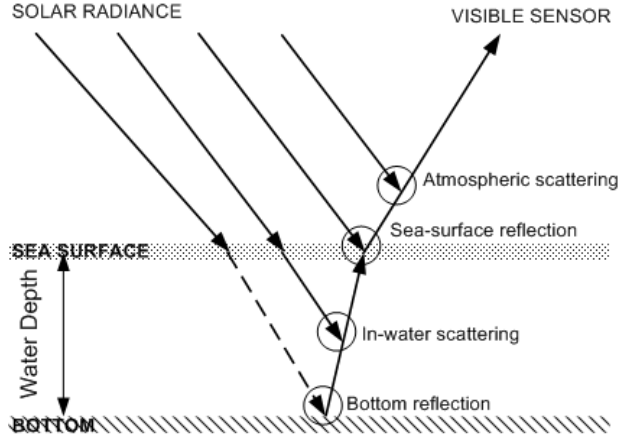


Figure 2. The elements of spectral radiance measured by sensor in water area; modified from Kanno (2011)

3.2 Modeling of Bathymetry

SDB model from remote sensing image works with an assumption that there is a linear relation between depth and water leaving radiance recorded by sensors. When the depth increases, the water leaving radiance decreases simultaneously until reaching a level at which bottom reflection is zero or undetectable as occur in the deep water area (Chénier et al., 2018). In this study, to extract depth information from remote sensing images as in Table 1, we used semi-parametric regression using spatial coordinate that was developed by (Kanno et al., 2011a). We compared the capability of SDB model derived from this algorithm with other method: multiple linear regression (Clark et al., 1987; Hamilton et al., 1993).

Semi-parametric regression using spatial coordinates (GAM): This method is actually the extension of Lyzenga’s method (Lyzenga, 1978) by combining it with a spatial interpolation method. It was developed by Kanno et al. (2011a) by modeling error term in Lyzenga’s method based on spatial dependency called semi-parametric regression. The formula can be written as (Kanno et al., 2011a; Kanno et al., 2011b):

$$h = X\beta + t(z) + \varepsilon' \quad (3)$$

where X and β are the Lyzenga’s estimators derived from SBES measurements and visible band of images. Meanwhile, $t(z)$ is a smooth nonparametric function of the two-dimensional coordinate vector z and ε' is a zero mean random variable. Penalized thin-plate regression spline was used when performing the equation. It is available in ‘mgcv’ package, especially the Generalized Additive Model (GAM) smoothing function. This package is available in ‘R’ software. Therefore, for the rest of the manuscript, we used the term ‘GAM’ for this method. Furthermore, in this experiment, we used the smooth term function ‘s’ which was optimized by Generalized Cross Validation (GCV) and regression ‘splines’ with fixed degrees of freedom. The critical step in implementing the SDB model is in defining this degree of freedom which is written as k . Based on Wood (2017), the value of k should not be too large or too small either. In this experiment we set various k values, for i.e., 100, 200, 400, 600, 800 and 1000. We evaluated the results by checking the RMSE value resulted by the model. Detailed explanations of this algorithm are available in Pya and Wood (2016) and Wood (2017).

Multiple Linear Regressions (MLR): Many previous studies used MLR for the extraction of bathymetry data using multispectral bands in shallow water (Clark et al., 1987; Hamilton et al., 1993). Van Hengel and Spitzer (1991) suggested that this method works by an assumption that the bottom reflectance and water composition are constant within all part of the image. Further, he said that multispectral bands of the imagery are affected by the bottom reflectance. By implementing this algorithm, the echo sounding measurement data is considered as the dependent variable. The transformed radiance Y_i is considered as the independent variable. The dependent variable, in this case, in situ data was used to determine the regression coefficient and estimates the depth information in shallow water area. The water depth can be estimated using the following equation (Van Hengel and Spitzer, 1991):

$$W_d = \beta_0 + \beta_1 Y_1 + \beta_2 Y_2 + \dots + \beta_n Y_i \quad (4)$$

where Y_1, Y_2, \dots, Y_i are the transformed radiance derived from Equation 2 for each band, β_0 is representing the y-intercept, while $\beta_1, \beta_2, \dots, \beta_i$ are slope for each band. These β -coefficients are obtained from the multiple linear

regressions with echo-sounding points. For this research, we set standard parameter when applying the algorithm.

3.3 Assessment of SDB models

To evaluate the results of bathymetry model, we assessed the accuracy by comparing the SDB data generated by the SDB model and the in situ measurements. For this purpose, we used 75% of SBES points as testing data and calculated the accuracy by using statistic model, the Root Mean Square Error (RMSE) shown in Equation 5.

$$RMSE_{(depth)} = \sum \sqrt{\frac{(X_i - X'_i)^2}{N}} \quad (5)$$

where X_i is the actual depth value (from validation set), X'_i is the expected value of SDB, and N is the number of elements in the data. Not only we calculated an overall RMSE value, but we calculated also the RMSE for five depth ranges, namely 0-5 m, 5-10 m, 10-15 m, 15-20 m, and 20-30 m. The aim was to find the most optimum depth for the SDB model.

4. RESULTS

4.1 Generalized Adaptive Model

From Figure 3a, we can see that $k = 1000$ obtained the lowest RMSE values implying the best performance of this model with R^2 equal to 0,977. By using the lowest k equal to 100, we obtained lower R^2 up to 0.951. Furthermore, it is obvious that by using $k = 1000$, image Kompsat-3 performed better than WorldView-2 and Landsat 8 OLI/TIRS performed better than Sentinel 2A. As an overall, Kompsat-3 provides the best accuracy of SDB model by using GAM.

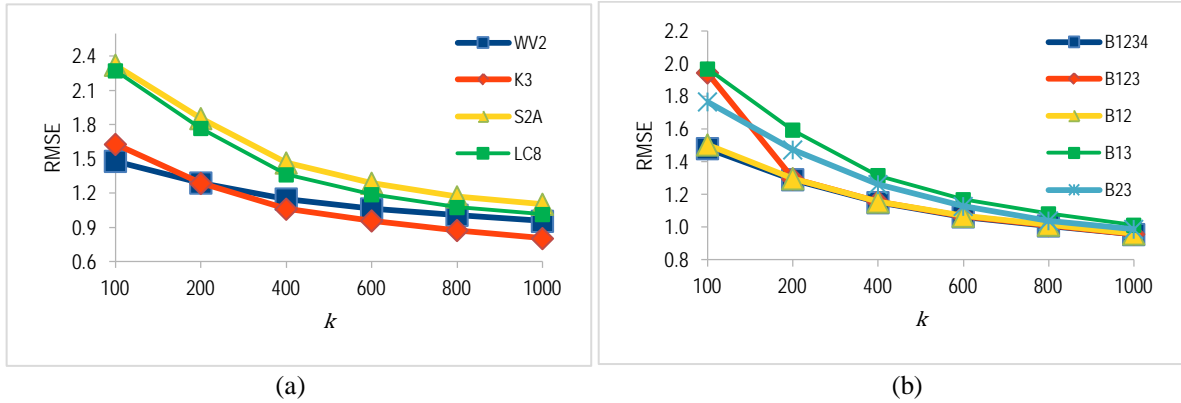


Figure 3. The RMSE value when applying GAM for: (a) four different sensors (using four bands: red, green, blue and NIR), namely: WW2=Worldview-2, K3=Kompsat-3, S2A=Sentinel 2A, and LC8=Landsat 8 OLI/TIRS; (b) five band combinations (B=band, 1=blue, 2=green, 3=red, and 4-NIR) of Worldview-2

Table 2. The accuracy of SDB Model using GAM applying to five datasets of WorldView-2 with various band combinations (see notations in Figure 3 for image band used). Asterisk symbol shows the best accuracy obtained for each band combination.

k	Band combinations				
	B1234	B123	B12	B13	B23
100	1.481	1.944	1.504	1.968	1.767
200	1.291	1.296	1.297	1.594	1.473
400	1.151	1.155	1.155	1.316	1.261
600	1.064	1.067	1.068	1.169	1.128
800	1.009	1.011	1.014	1.082	1.039
1000	0.956*	0.958*	0.960*	1.013*	0.987*

When we compare GAM performance applying at five different band combinations of WorldView-2, combination using four bands is only slightly better than other combinations such as three bands and two bands. From the experiment, combination of blue-green bands produced slightly better result than combination of blue-

red and green-red bands.

4.2 Multi Linear Regression

From Figure 4 and Table 3, we can see that SDB model using four bands of WorldView-2 produced the best accuracy with R^2 equal to 0.91, whereas, RMSE value of SDB models using Kompsat-3 with four and three bands only differ little with $R^2 > 0.85$. Surprisingly, when using Sentinel 2A and Landsat 8 OLI/TIRS for SDB model, dataset with two bands, specifically red-green bands provided the best RMSE result. From Figure 4, it is obvious that WorldView-2 gives the best performance in generating SDB model, followed by Kompsat-3. In this case, the SDB results were significantly influenced by spatial resolution of data that were used.

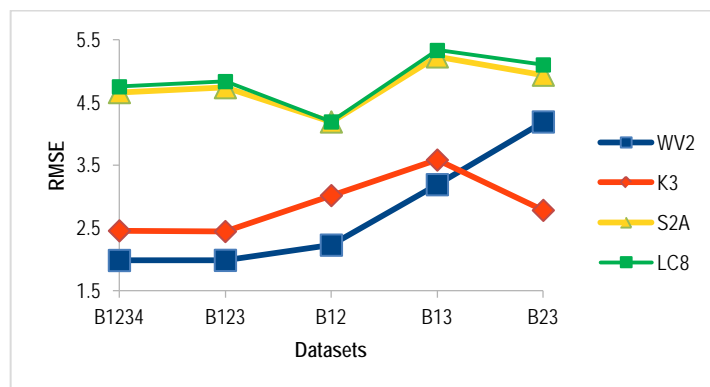


Figure 4. The RMSE value when applying MLR for four different sensors, namely: WV2=Worldview-2, K3=Kompsat-3, S2A=Sentinel 2A, and LC8=Landsat 8 OLI/TIRS and using five band combinations (B=band, 1=blue, 2=green, 3=red, and 4=NIR)

Table 3. The accuracy of SDB Model using MLR applying to five datasets with various band combinations (see notations in Figure 3 for image band used and name of satellite images). Asterisk symbol shows the best accuracy obtained for each band combination.

Bands	Sensors			
	WV2	K-3	S2A	LC8
B1234	1.989*	2.461	4.661	4.752
B123	1.991	2.450*	4.739	4.836
B12	2.233	3.022	4.193*	4.193*
B13	3.195	3.587	5.229	5.331
B23	4.193	2.787	4.938	5.101

4.3 Comparison of the Models

A comparison of RMSE value for each depth range is presented in Figure 5. By comparing the SDB models by using four bands of images (red, green, blue, and NIR bands), in general, both models are perform well in all depth range. However, by using GAM method, WorldView-2, Sentinel 2A and Landsat 8 OLI/TIRS performed better in shallow water area at depth range 0-5 than other depth ranges. This is supported by information provided in Figure 6. The scatter plots in Figure 6(a,c,d) show that the actual depth data from in situ measurement and SDB model fits better at the shallow water area (0-5 m). While Kompsat-3 performed slightly better in deep area at depth range 20-30 m as also supported by Figure 6b. By using MLR method, the optimum depth for Worldview-2 is at depth range 0-5 m, while for other images, they performed slightly better at depth range 10-15 m than other depth ranges.

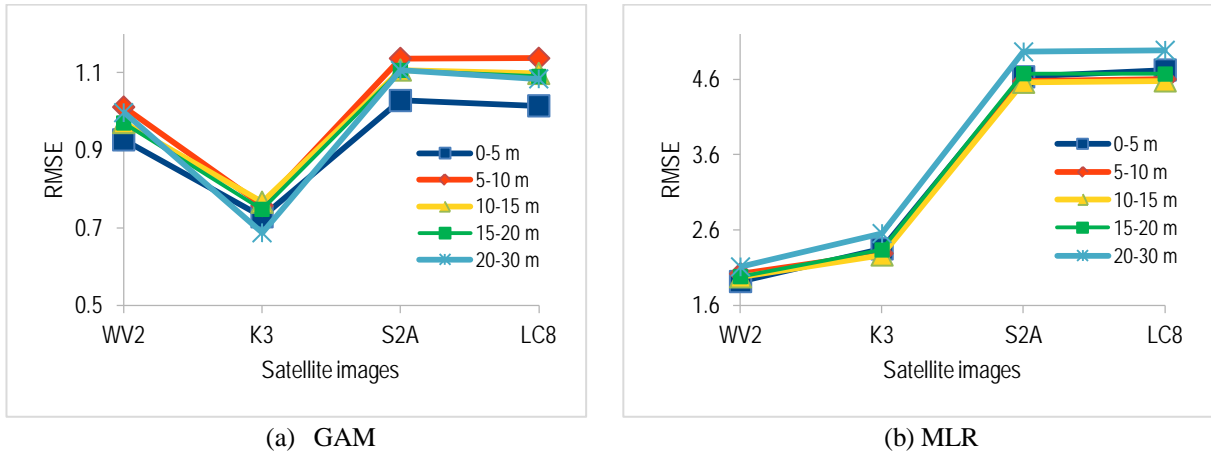


Figure 5. The RMSE value when applying GAM and MLR at various depth ranges for four different sensors using four bands (red, green, blue and NIR) (see notations in Figure 3 for name of satellite images).

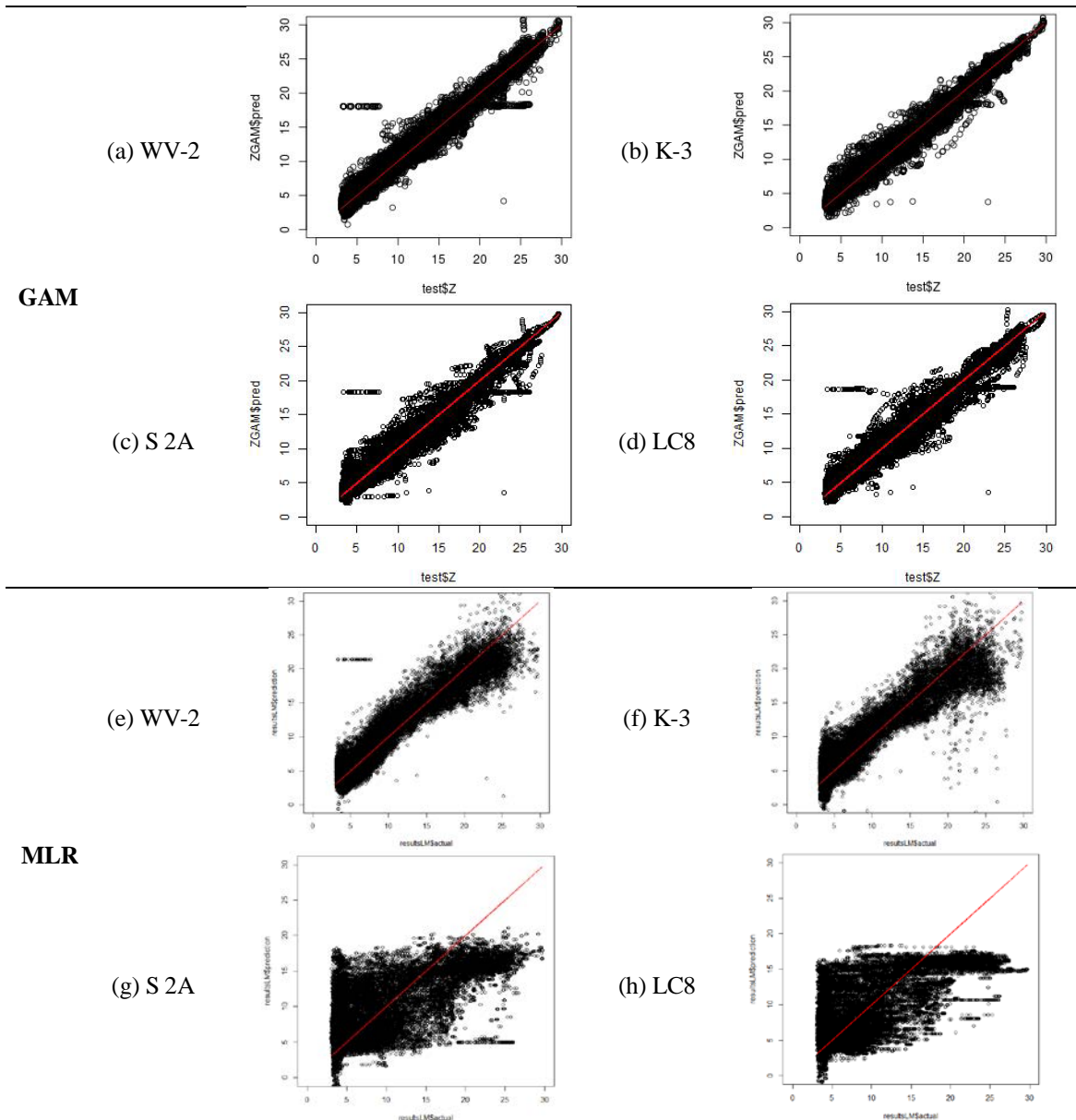


Figure 6. Validation plots of depth model when applying GAM and MLR using four different sensors using four bands (red, green, blue and NIR). The size of validation set is 75% of all in situ measurements.

5. DISCUSSIONS

In general, using more bands (three and four bands) provide a better result, especially when using MLR as described by Bramante et al. (2013) the number of bands used in the model is related to the capability of the algorithm to discriminate different bottom types and water masses, thus more bands may produce a more accurate. However, GAM model was not greatly influenced by the number of bands when performing SDB model (see Table 2). On the other hand, using only two bands (specifically red-green bands) for SDB models was also promising, especially when using Sentinel 2A and Landsat 8 OLI/TIRS (see Table 3).

Our results demonstrated the outperformance of GAM compared to MLR as also proved by Kanno et al. (2011a). The inclusion of spatial coordinates in GAM model could improve the accuracy of SDB model. For example for WorldView-2 images, by using GAM, the accuracies range from 0.9-1.9 while by using MLR model, the accuracies range from 1.9-5.3.

The results also show that the use of finer resolution images such as Kompsat-3 and WorldView-2 improved the SDB accuracies. In fact, a decrease in image spatial resolution affects spectral heterogeneity of the image since it causes mixed pixels (see visual comparison in Figure 7). However, there were unexpected results such as the fact that Landat 8 OLI/TIRS with 30 m spatial resolution outperformed SDB model using Sentinel 2A which has finer resolution (10 m). This could be due to the spectral reflectance variations of the images captured by different sensors. It might occur that by using GAM, coarser resolution has less noise. Besides, it may also probably due to the presence of pixels with no data (see Figure 7c,g) implying a comprehensive atmospheric and water column correction is needed.

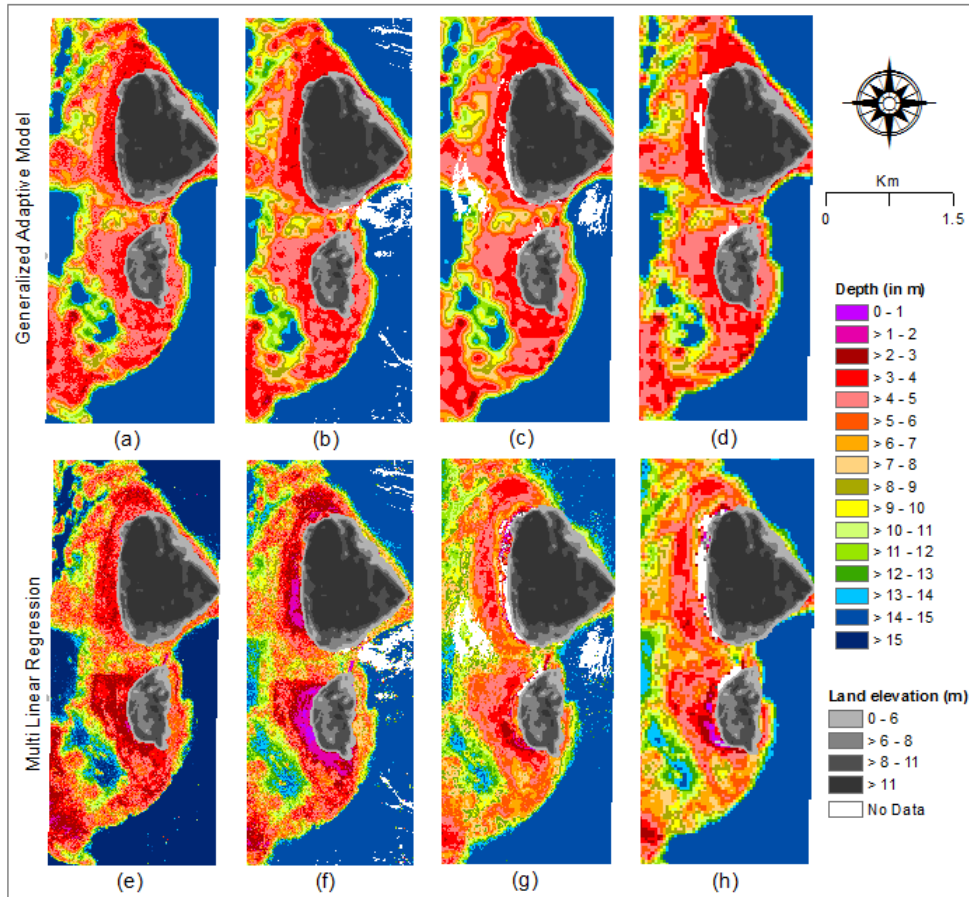


Figure 7. Comparison of SDB model resulted by applying GAM and MLR for four datasets (a,e) WorldView-2, (b,f) Kompsat-3, (c,g) Sentinel 2A, and (d,h) Landsat 8 OLI/TIRS. Each image consists of four bands and for applying GAM, we set $k = 1000$. Land elevations were derived using DEMNAS elevation data from BIG (2018)

CONCLUSIONS

This research provides a comparative analysis of two bathymetry models by applying both models to four different satellite images and band combinations. GAM model obtained better results than MLR and among four satellite images; Kompsat-3 produced the best accuracy of SDB model when using GAM, and WorldView-2 obtained the best accuracy when using MLR. Integration of more bands to the SDB models proved to an improved accuracy. However, when only using two bands, combination of red and green bands showed the best performance. Further study is needed to evaluate other possible band combinations which can improve the accuracy.

REFERENCES

- BIG (2018). DEMNAS: Seamless Digital Elevation Model (DEM) dan Batimetri Nasional. In. Cibinong, Indonesia: Geospatial Information Agency (Badan Informasi Geospasial)
- Bramante, J.F., Raju, D.K., Sin, T.M. (2013). Multispectral derivation of bathymetry in Singapore's shallow, turbid waters. *International Journal of Remote Sensing*, 34, 2070-2088
- Chénier, R., Faucher, M.-A., Ahola, R. (2018). Satellite-Derived Bathymetry for Improving Canadian Hydrographic Service Charts. *ISPRS International Journal of Geo-Information*, 7
- Clark, R.K., Fay, T.H., Walker, C.L. (1987). Bathymetry calculations with Landsat 4 TM imagery under a generalized ratio assumption. *Applied Optics*, 26, 4036_4031-4038
- DigitalGlobe (2013). DigitalGlobe's Core Imagery Product Guide. In (p. 49)
- DigitalGlobe (2019). Standard Imagery. In (p. 2). London: Digital Globe
- ESA (2015). Sentinel-2 Products Specification Document. In. France: ESA
- ESA (2019). Copernicus In
- Gholamalifard, M., Esmaili Sari, A., Abkar, A., Naimi, B. (2013). Bathymetric Modeling from Satellite Imagery via Single Band Algorithm (SBA) and Principal Components Analysis (PCA) in Southern Caspian Sea. *Int J Remote Sens*, 7, 877-886
- Hamilton, M.K., Davis, C.O., Rhea, W.J., Pilorz, S.H., Carder, K.L. (1993). Estimating chlorophyll content and bathymetry of Lake Tahoe using AVIRIS data. *Remote Sensing of Environment*, 44, 217-230
- Hengky, S.H. (2017). Gazing Coastal Ecotourism in Morotai Islands, Indonesia. *Environmental Management and Sustainable Development*, 6
- Kanno, A. (2011). Shallow Water Bathymetry from Multispectral Satellite Images: Extensions of Lyzenga's Method for Improving Accuracy. *Coastal Engineering Journal*, 53, 431-450
- Kanno, A., Koibuchi, Y., Isobe, M. (2011a). Shallow Water Bathymetry from Multispectral Satellite Images: Extensions of Lyzenga's Method for Improving Accuracy. *Coastal Engineering Journal*, 53, 431-450
- Kanno, A., Koibuchi, Y., Isobe, M. (2011b). Statistical Combination of Spatial Interpolation and Multispectral Remote Sensing for Shallow Water Bathymetry. *IEEE GEOSCIENCE AND REMOTE SENSING LETTERS*, 8, 64-67
- Kanno, A., Tanaka, Y., Kurosawa, A., Sekine, M. (2013). Generalized Lyzenga's Predictor of Shallow Water Depth for Multispectral Satellite Imagery. *Marine Geodesy*, 36, 365-376
- KARI (2015). Kompsat-3 Product Specification. In (p. 51). South Korea: SI Imaging Services
- Lyzenga, D.R. (1978). Passive remote sensing techniques for mapping water depth and bottom features. *Applied Optics*, 17, 379-383
- Lyzenga, D.R. (1981). Remote sensing of bottom reflectance and water attenuation parameters in shallow water using aircraft and Landsat data. *Int J Remote Sens*, 2, 71-82
- Pattanaik, A., Sahu, K., Bhutiyani, M.R. (2015). Estimation of Shallow Water Bathymetry Using IRS-Multispectral Imagery of Odisha Coast, India. *Aquatic Procedia*, 4, 173-181
- Philpot, W.D. (1989). Bathymetric mapping with passive multispectral imagery. *Applied Optics*, 28, 1569-1578
- Pya, N., Wood, S.N. (2016). A note on basis dimension selection in generalized additive modelling. In. USA: Cornell University
- Saputro, G.B., Hartini, S., Dartoyo, A.A., Setyawan, I.E., Wijaya, S.W., Subagyo, H., Idrus, I.N., Yuwono, D.M. (2012). Pulau Morotai: Sumberdaya Strategis di Kawasan Timur Indonesia. (2nd ed.). Cibinong, Indonesia: BAKOSURTANAL
- Stumpf, R.P., Holderied, K., Sinclair, M. (2003). Determination of water depth with high-resolution satellite imagery over variable bottom types. *Limnology and Oceanography*, 48, 547-556
- SUHET (2015). Sentinel-2 User Handbook. In (p. 64): ESA
- USGS (2019a). Landsat 8 (L8) Data Users Handbook. In. South Dakota, USA: Department of the Interior USGS
- USGS (2019b). USGS EarthExplorer. In
- Van Hengel, W., Spitzer, D. (1991). Multi-temporal water depth mapping by means of Landsat TM. *International Journal of Remote Sensing*, 12, 703-712

- Vinayaraj, P., Raghavan, V., Masumoto, S. (2016). Satellite-Derived Bathymetry using Adaptive Geographically Weighted Regression Model. *Mar. Geod.*, 39, 458–478
- Wood, S.N. (2017). *Generalized Additive Models: An Introduction With R.* (Second Edition ed.). Boca Raton: CRC